Volume 42, Issue 3, March 2007 ISSN 0360-1323

BUILDING AND ENVIRONMENT

The International Journal of Building Science and its Applications

Editor: E. H. MATHEWS
North West University, R.S.A.

Available online at
ScienceDirect
www.sciencedirect.com

Available online at www.sciencedirect.com
ScienceDirect
Building and Environment 42 (2007) 1142–1150
BUILDING AND ENVIRONMENT
www.elsevier.com/locate/buildenv

Scale model study of airflow performance in a ceiling slot-ventilated enclosure: Non-isothermal condition

Hsin Yu[a], Chung-Min Liao[b,*], Huang-Min Liang[b], Kuo-Chih Chiang[b]

[a]*Department of Civil Engineering, National Ilan University, Ilan 260, Taiwan ROC*
[b]*Department of Bioenvironmental Systems Engineering, National Taiwan University, Taipei 10617, Taiwan ROC*

Received 16 August 2005; accepted 4 December 2005

Abstract

Scale-model study of a non-isothermal ceiling slot-ventilated enclosure was investigated in both airspeed and thermal fields. Results of airflow pattern, centerline velocity and centerline temperature decay, velocity and temperature profile, airflow boundary layer and thermal boundary layer growth, floor velocity, and floor temperature difference were analyzed to establish semi-empirical prediction equations. Results also compared with previous researches to validate the physical behavior of air-jet. Data of centerline velocity decay showed similar airflow characteristics as isothermal air-jet with Archimedes number (Ar) <0.004, which performed as pseudo-isothermal airflow. Air-jet fell on entry with $Ar>0.018$. A single circulation airflow existed at $0.004<Ar<0.011$ and two-circulation airflow occurred at $0.011<Ar<0.018$. The centerline velocity decay was fitted well as similar form of an isothermal condition. The centerline temperature decay was fitted well as the form of centerline velocity decay in both ceiling and floor regions. Both the velocity and temperature profiles agreed with results obtained from literature. Both airflow boundary layer and thermal boundary layer growths increased with traveling distance of air-jet. Maximum floor velocity and floor temperature difference were fitted well with different parameters. Analysis of airflow performance in a non-isothermal condition makes progress in predicting air quality inside the enclosures and guides the design concepts of ventilation system for an indoor environment.

Keywords: Airflow characteristics; Slot-ventilated; Ventilation; Non-isothermal; Archimedes number

1. Introduction

Airflow characteristics inside room affect the air distribution, the thermal environment, and the contaminant concentrations. It also determinates the distribution of thermal energy, moisture, and fresh air into a room. Airflow characteristics are dominated by the behavior of inlet air-jet. Air-jet is used to mix inlet air with room air in most mechanically ventilated enclosures. The theoretical and experimental investigations of confined plane wall jet is much more difficult than the free plane wall jet [1]. On the other hand, the study of non-isothermal airflow in a ventilated enclosure is more close to the reality than in isothermal condition.

The purpose of this study is to analyze air-jet characteristics in non-isothermal slot-inlet ventilated enclosures by experimental processes. Measurements of airspeed and temperature fields associated with airflow trajectory visualization have been investigated in scale-model. The centerline velocity and centerline temperature decays, growths of airspeed and temperature profiles, velocity and temperature profiles as well as flow velocity and temperature distribution were analyzed through experimental determination and compared with theoretical results from literature. Semi-empirical equations were established to describe the airflow characteristics in a non-isothermal condition. Performance of a non-isothermal air-jet in ceiling slot-ventilated enclosure would be predicted by the analysis of airflow characteristics and offer a suggestion of design guidelines of ventilation system for controlling indoor environment.

*Corresponding author. Tel.: +886 2 23634512; fax: +886 2 23626433.
E-mail address: cmliao@ntu.edu.tw (C.-M. Liao).

0360-1323/$ - see front matter © 2006 Elsevier Ltd. All rights reserved.
doi:10.1016/j.buildenv.2005.12.004

Nomenclature

Ar	Archimedes number
Ar_c	corrected Archimedes number
Ar_w	wall jet Archimedes number
C_d	diffuser discharge coefficient
g	gravitational acceleration rate ($m\,s^{-2}$)
h	diffuser width (m)
H	room height (m)
J	jet momentum number defined as $\frac{QU_d}{gV}$
K_1	airspeed decay constant
K_2	temperature decay constant
L	room length (m)
L_p	penetration distance defined by Adre and Albright [6] (m)
M	momentum of jet defined as $\rho h U_d^2$ per unit length of diffuser ($N\,m^{-1}$)
Pr	Prandtl number defined as $\frac{\alpha}{\nu}$
Q	ventilation rate ($m^3\,s^{-1}$)
Re	Reynolds number, defined as $\frac{hU_d}{\nu}$
Rm	inlet jet momentum ratio defined as $hU_d^2/(L+H)(m^2\,s^{-2})$
T	mean temperature (°C)
ΔT	temperature difference between floor and outdoor (°C)
U	mean air velocity ($m\,s^{-1}$)
w	diffuser length (m)
W	room width (m)
x	horizontal distance from inlet wall (m)
y	vertical distance from floor (m)
$y_{0.5t}$	location where $T_r - T = (T_r - T_m)/2$(m)
$y_{0.5v}$	location where $U = U_m/2$(m)

Greek letters

α	thermal diffusion coefficient ($m^2\,s^{-1}$)
β	thermal expansion coefficient defined as $\frac{1}{(T_f+T_d)/2}(K^{-1})$
η_t	ratio of y to $y_{0.5t}$
η_v	ratio of y to $y_{0.5v}$
ν	kinematic viscosity ($m^2\,s^{-1}$)

Subscripts

d	diffuser
f	floor
m	maximum of inertia flow
r	room, ambient
rm	maximum of reverse flow
t	terminal value
w	wall

2. Theoretical background

2.1. Airflow pattern

Representations of the separation distance of linear jet or impingement distance from inlet wall were related to Archimedes number $Ar = \beta g h(T_f - T_d)/U_d^2$ [2–5]. Air-jet penetration has been used to express airflow patterns quantitatively. Adre and Albright [6] defined air-jet penetration (L_p) as the distance from the inlet wall where the wall jet separated from the ceiling. Kaul et al. [7] defined air-jet penetration as the distance from the inlet wall on the floor where the incoming air-jet impinged (L_{pn}).

Randall and Battams [8] conducted stability criteria for airflow patterns in livestock buildings using a prototype building with heated cylinders simulating pigs. They proposed an inlet corrected Archimedes number $Ar_c = C_d g w h W H(W+H)(T_f - T_d)/((546 + T_f + T_d)Q^2))$ to describe the relative influence of buoyant forces on the air-jet. Their results showed that the air-jet remained horizontal for Ar_c less than 30 and fell immediately to the floor when it was greater than 75. Wang and Ogilvie [9] investigated airflow patterns in slot-ventilated rooms under non-isothermal conditions using a test room where the room height was varied. A wall jet Archimedes number $Ar_w = \beta g(T_f - T_d)HL/(hU_d^2)$ was defined and proposed as the criterion describing airflow patterns. The Ar_w was about 40 before the air-jet extended to the midpoint of the room and was about 110 for fully rotary airflow. A significant lag phenomenon was found in the study where once a fully rotary airflow pattern was created; the inlet velocity could be decreased significantly without changing the airflow pattern with the Ar_w increased to about 240. Zhang [10] described this lag phenomenon in a study of the relation between the horizontal air-jet penetration and the diffuser air velocity for non-isothermal airflow. It concluded that extra momentum was needed to overcome the existing airflow pattern before a new flow pattern could be formed. The critical Ar defined as the condition where the air-jet fell on entry was found for non-isothermal airflow.

2.2. Centerline velocity decay and centerline temperature decay

The expression of centerline velocity decay in a non-isothermal enclosure had similar form as in an isothermal condition [3,4,11,12]. The normalized extreme airspeed was reverse related to the normalized distance from diffuser as $U_m/U_d \propto \sqrt{h/x}$, where the related coefficient between the two variables was usually referred to as the throw constant [13] or velocity decay constant [4], and the value varied in

different literature. Hassani et al. [3] found that the K_1 value in the equation of centerline velocity decay was not significantly different between isothermal and non-isothermal jets and did not depend on temperature.

The expression of centerline temperature decay [3,4,12] had the similar form as of centerline velocity decay, that was $(T_r - T_m)/(T_r - T_d) \propto \sqrt{h/x}$. The related temperature decay constant (K_2) dominated the variation between normalized temperature difference and the normalized distance from opening. Hassani et al. [3] pointed out that the temperature decay constant was less than the velocity decay constant as $K_2 \approx 0.85 K_1$.

2.3. Velocity profile and temperature profile

The expression of velocity profile for plane wall jet in a non-isothermal enclosure [12,14,15] was different with those described in an isothermal condition [16]. The variables of these equations were related to the ratio of $y/y_{0.5t}(\eta_t)$ or $y/y_{0.5v}(\eta_v)$ along vertical distance in different studies. The equations of temperature profile for plane wall jet in a non-isothermal enclosure expressed similar form as of velocity profile [12,14,15]. Yet the value of coefficient or exponential power was different.

2.4. Airflow boundary layer growth and temperature boundary layer growth

The expressions of airflow boundary layer growth were of the form as $dy_{0.5v}/dx = C$, where C ranged from 0.065 to 0.1 [16,17]. The spread angle of the plane wall jet was about 10–12° that is half value of a free wall jet [18]. All results were derived from research of isothermal condition because of that no airflow boundary layer growth in non-isothermal condition was found depending on the efforts in this project. Wilson et al. [14] derived a simple expression of thermal boundary layer growth that was related to the traveled length of jet and Ar. The regression equation of C in Wilson et al. [14] was derived by this project to find the variation of coefficient in different Ar.

2.5. Floor velocity

Zhang et al. [11] derived averaged reverse flow velocity of occupied zone related with Ar when Reynolds number Re remains constant. Wang and Ogilvie [9] showed that the mean floor velocity and maximum floor velocity can be expressed related to momentum ratio (Rm) and $H\Delta T$ in two different configurations of scale model, which is inlet and outlet at same wall and the other is at opposite wall. The results also showed that the floor velocity measured in the case of inlet and outlet at opposite wall is lower (20% less) than that measured in the case which inlet and outlet at same wall. When the air-jet passed over the outlet area, the inner layer of the airflow would be affected by the suction effect and cause significant jet momentum loss [9].

3. Materials and method

Airflow performance and thermal characteristics of plane wall jet in ceiling slot-ventilated enclosure under a non-isothermal condition was investigated by experimental measurement. A scaled model of 1:3 representing a prototype building was used to study airflow performance in a confined enclosure. Anemometer and temperature instruments measured the airflow characteristics of velocity fields and thermal fields inside an enclosure. The configuration and dimensions of the test chamber used is shown in Fig. 1. Slot inlet width (w) is the same as width of the enclosure (W). As a result of the inlet aspect ratio been much greater than 20, resulting the airflow was treated as a two-dimensional wall jet without the effect of sidewalls [19]. The scale model was constructed of 12.7 mm thick plywood. The inner surfaces were sanded and painted black. The front wall was made of Plexiglas to accommodate airflow visualization. Access holes were placed on the top ceiling between inlet wall and end wall at intervals of 20 mm, except for the area between the inlet and a distance of 33 h from the inlet where a continuous access slot was constructed to discretize air-jet development near the inlet.

Ductwork was constructed and fitted between the circular exhaust hole and an exhaust fan (Model 3C507A; Dayton Electric MFC, Co.). Calibrated orifice plates were used to select desired airflow rates through model. A micro-manometer (Model 1430; Dwyer Instruments, Inc.) was used to measure the pressure difference across the orifice to determine airflow rate. The orifice plates used in the pressure measurements were calibrated by a standard Venturi flow meter. The calibration curve showed good correlation with $r^2 > 0.99$. The floor of model was fitted with insulated silicone rubber heat panels (Model SRFG 442/2 and 1242/2; OMEGA Engineering, Inc.) that occupied 58% of the floor area to simulate occupied surface temperature. The power density was 3875 (W m^{-2}) and was controlled by miniature microprocessor temperature controllers (Model CN9000; OMEGA Engineering, Inc.) with an accuracy of ±0.5 °C using a PID control

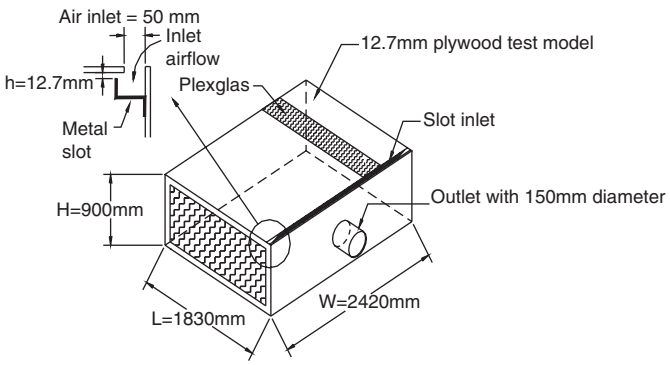

Fig. 1. Schematic showing the dimensions of experimental scale-model.

Table 1
Test conditions of experimental measurement for non-isothermal airflow

Test	Q (cms)	U_d (m s^{-1})	T_d (°C)	T_f (°C)	ΔT (°C)	Re	Rm	Ar	Ar_c
NP1	0.153	4.97	61.5	21.5	40	3976	0.115	0.0006	4
NP2	0.104	3.39	61.5	21.5	40	2708	0.053	0.0014	8
NP3	0.071	2.30	57	17	40	1842	0.025	0.0030	18
NP4	0.050	1.61	57.5	17.5	40	1284	0.012	0.0062	37
NP5	0.034	1.10	54.5	14.5	40	882	0.006	0.0133	80
NP6	0.027	0.90	55.5	15.5	40	716	0.004	0.0201	121
NP7	0.025	0.81	62.77	22.77	40	649	0.003	0.0239	144
NP8	0.055	1.78	82.33	22.33	60	1424	0.015	0.0072	44
NP9	0.039	1.28	79.37	19.37	60	1025	0.008	0.0141	85
NP10	0.034	1.12	81.94	21.94	60	898	0.006	0.0182	110
NP11	0.028	0.90	79.56	19.56	60	723	0.004	0.0283	170

mode. The maximum operating temperature of the heaters was 120 °C.

Airspeed was measured using an omni-directional hot-film anemometer (Model 8470; TSI, Inc.) that was calibrated by the manufacture. The % error was below 3%. A portable data acquisition system (Model CR10; Campbell Scientific, Inc.) was used to collect data. The average over time, at a point, was used for analysis and presentation. The acquiring period for each point was fixed to 180 s and the sampling frequency was set at 16 Hz to ensure accurate time-average results for turbulent airflow [20]. The temperature field was measured using T-type thermocouples connected to the same data acquisition system as the airspeed measurements. Both the inertia and buoyant forces affect the airflow pattern in a non-isothermal enclosure. Several airflow rates were chosen to encompass the anticipated stable and unstable airflow zones. Table 1 lists the test conditions for quantifying the airflow pattern.

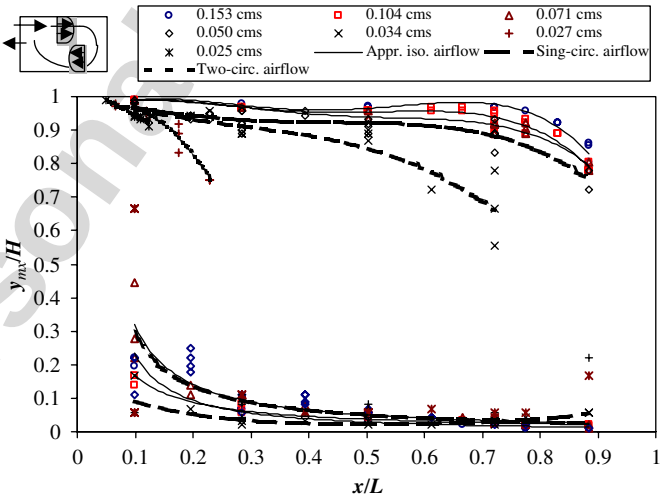

Fig. 2. Normalized peak airspeed trajectory in a non-isothermal enclosure at $\Delta T = 40$ °C.

4. Results and discussion

4.1. Airflow pattern

Airflow patterns were observed by visualization of centerline velocity trajectory as represented by various airflow rates with $dT = 40$ °C (Fig. 2). The airflow penetration distance was decided when the centerline of air-jet fall to the height of $0.9H$. Fig. 3 presents the results of normalized penetration distance of air-jet versus Ar. The critical values measured and used to distinguish the behavior of non-isothermal air-jets are shown in the plot. At critical $Ar < 0.004$ ($Ar_c < 27$), a single-circulation airflow pattern with fully rotary existed and the airflow pattern was governed by the isothermal behavior. At critical $Ar > 0.018$ ($Ar_c > 110$), buoyant force dominated airflow performance and air-jet fell immediately after diffused on the entry. Critical values to distinguish the airflow pattern are similar to Randall and Battams [8] in the fully rotary

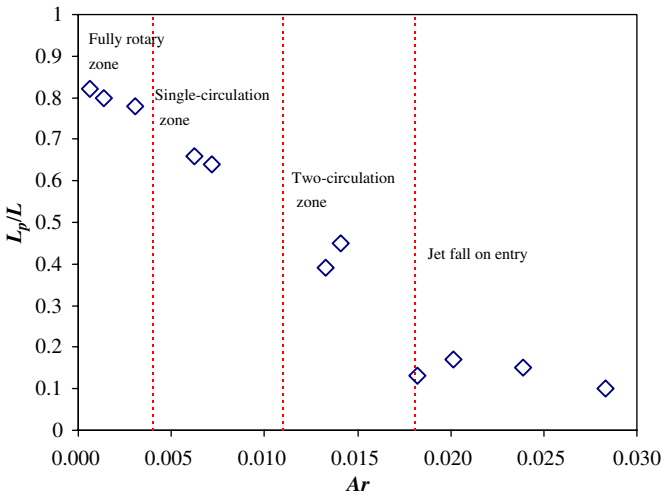

Fig. 3. Critical values to distinguish non-isothermal airflow patterns based on normalized air-jet penetration distance versus Archimedes number (Ar).

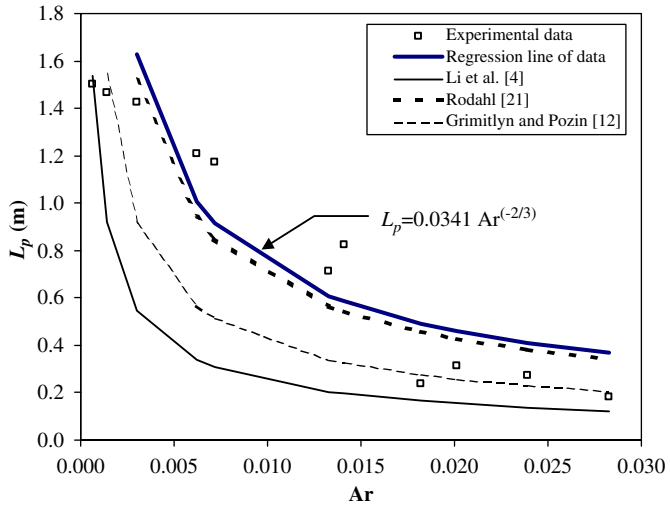

Fig. 4. Penetration distance of non-isothermal enclosure versus Archimedes number (Ar).

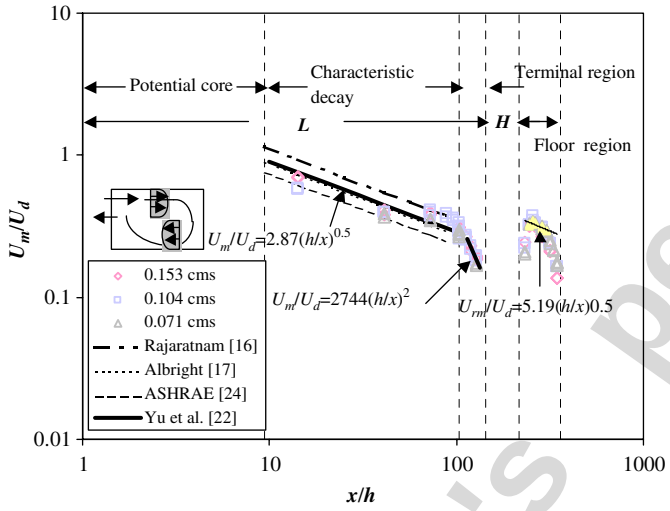

Fig. 5. Normalized centerline velocity decay along perimeter of non-isothermal enclosure.

condition (i.e., $Ar_c < 30$), and similar to Zhang [10] in the jet fall on entry (i.e., $Ar_c > 113$).

For intermediate range ($0.004 < Ar < 0.018$), the air-jet was unstable with single-circulation or two-circulation airflow type. The critical value to distinguish them is about $Ar = 0.011$ ($Ar_c = 72$) when the air-jet penetration distance beyond $x = 0.5L$. The penetration distance of intermediate range was fitted linearly as following (Fig. 4):

$$L_p = 0.0341\left(\frac{1}{Ar}\right)^{2/3}, \quad (r^2 = 0.81). \tag{1}$$

The expression is more similar to that of Rodahl [21] than that of Li et al. [4] and Grimitlyn and Pozin [12].

4.2. Centerline velocity decay and centerline temperature decay

The centerline velocity decay of air-jet was unstable when the airflow pattern was dominated by buoyancy or in an intermediate airflow condition (i.e., $Ar > 0.004$). The experimental data were fitted well in both ceiling and floor regions at $Ar < 0.004$ when fully rotary airflow was dominated by inertia force as in a pseudo-isothermal condition (Fig. 5). The centerline velocity decay of ceiling region in characteristic decay and terminal regions for non-isothermal plane wall jet can be simulated with same decay equations for an isothermal condition [22]. The equations were derived as following, respectively:

$$\frac{U_m}{U_d} = 2.87\sqrt{\frac{h}{x}}, \tag{2}$$

$$\frac{U_m}{U_d} = 2744\sqrt{\frac{h^2}{x^2}}. \tag{3}$$

The characteristic decay region was between the distance of $x = 10$ and $100h$. Beyond this distance, centerline velocity vanished rapidly in the terminal region. The decay of normalized centerline velocity has similar form as in previous studies [16,17,23].

Normalized centerline velocity in floor region was fitted well when the reversed air-jet traveled through floor surface as plane wall jet. Airspeed decay equation in characteristic decay region was expressed as

$$\frac{U_{rm}}{U_d} = 5.19\sqrt{\frac{h}{x}}. \tag{4}$$

The throw constant in a non-isothermal condition was less than the value in an isothermal condition (i.e., 3.73) [22]. It may result from that stronger buoyancy affects the decay rate in a non-isothermal floor region.

Data of centerline temperature decay in both ceiling and floor regions were fitted well (Fig. 6(A)). The temperature decay of ceiling region (Fig. 6(B)) in different airflow rates were fitted well within the characteristic decay region according to the form of previous studies [4,15,24] as following:

$$\frac{T_r - T_m}{T_r - T_d} = 2.44\sqrt{\frac{h}{x}}. \tag{5}$$

The temperature decay constant was chosen as $K_2 = 0.85K_1$ (i.e., $2.44 = 0.85 \times 2.87$) from Hassani et al. [3]. The normalized temperature difference decreased with the increasing normalized air-jet traveling distance. The cool diffused air-jet became warm when the hot entrainment of ambient room air mixed with the air-jet.

The centerline temperature decay within the terminal region had similar form as the centerline velocity decay as

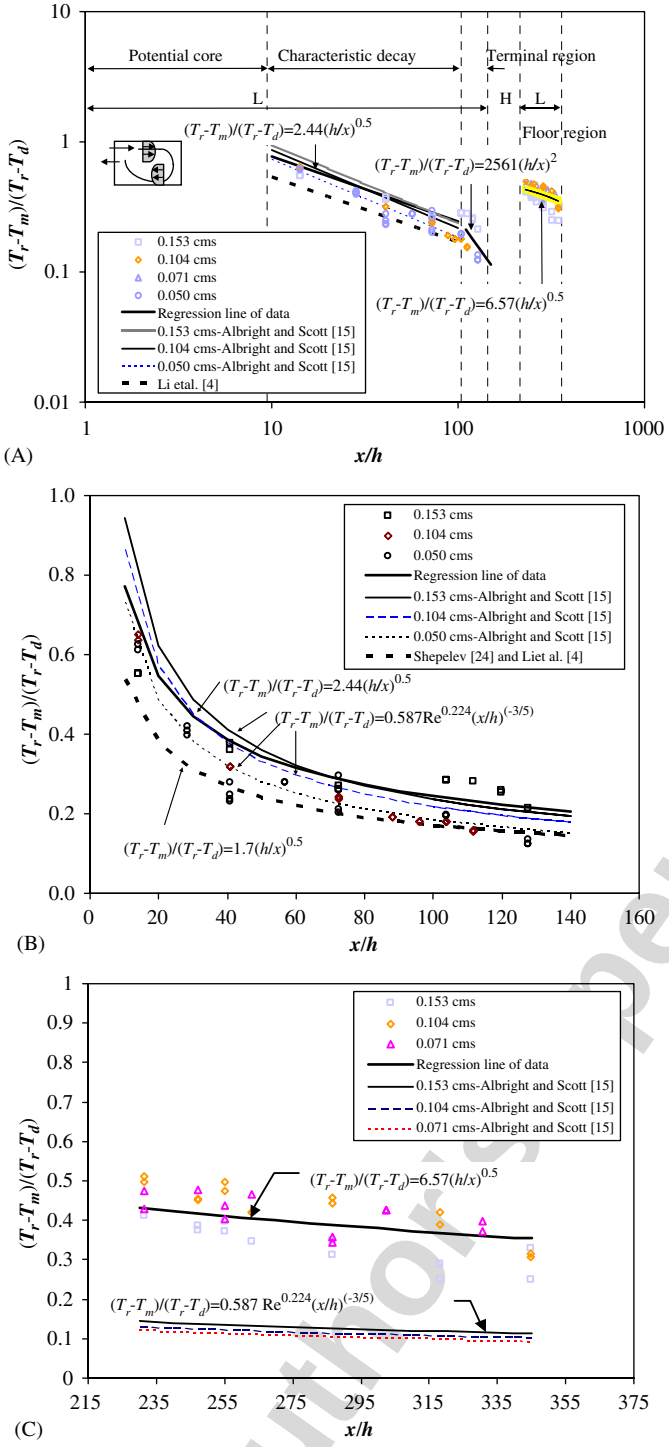

Fig. 6. Normalized centerline temperature decay (A) along perimeter, (B) along ceiling region, and (C) along floor region of non-isothermal enclosure.

following:

$$\frac{T_r - T_m}{T_r - T_d} = 2561\left(\frac{h}{x}\right)^2. \quad (6)$$

The variation of temperature decay for different airflow rates was not significant through floor region and can be

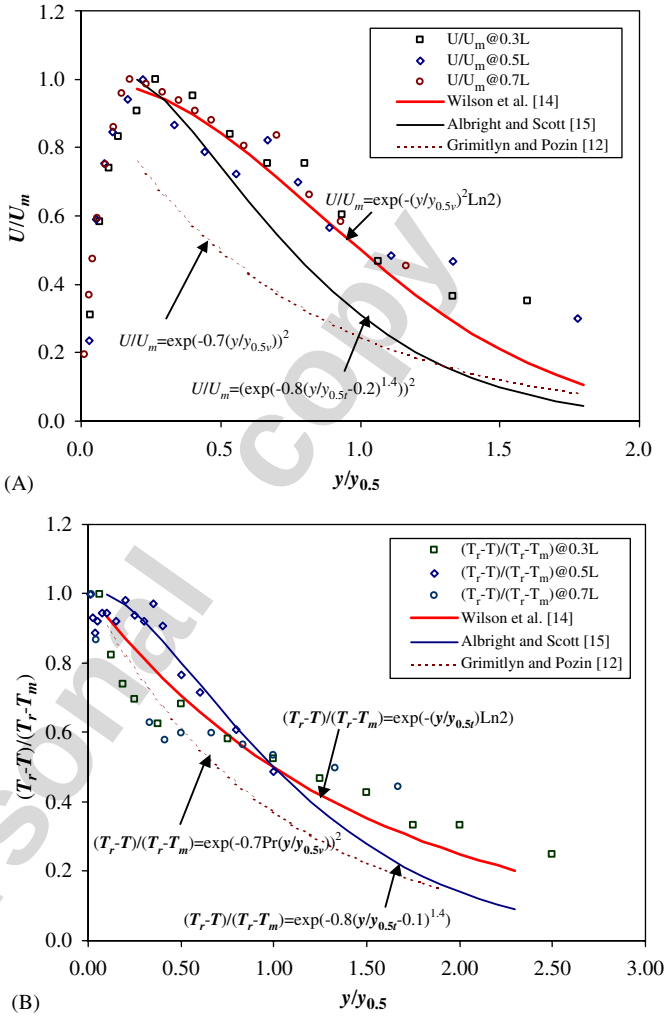

Fig. 7. (A) Normalized velocity profiles and (B) normalized temperature profiles of non-isothermal plane wall jet in ceiling region.

fitted by the similar form of ceiling region as following (Fig. 6(C)),

$$\frac{T_r - T_m}{T_r - T_d} = 6.57\left(\frac{h}{x}\right). \quad (7)$$

The heat exchange between cool inlet air and hot room air was mixed thoroughly when the air-jet impinged the floor region. The floor heater established much thermal capacity in the floor region that caused insignificant variation of temperature decay. The fitted equations of temperature decay in floor region were not approached to the form as of Albright and Scott [15] because their model is used in the ceiling region, but were similar to other studies.

4.3. Velocity profiles and temperature profiles

Normalized velocity profile of non-isothermal plane wall jet are conducted from different position (i.e., $x = 0.3$, 0.5, and $0.7L$) with airflow rate of 0.185 cms and $\Delta T = 40\,^{\circ}\mathrm{C}$ as

shown in Fig. 7(A). The predicted curves were derived from previous research which based on different variables of η_v or η_t. η_t is calculated from vertical distance of thermal boundary layer spread index ($y_{0.5t}$) [15], and η_v was based on the vertical distance of jet spread index ($y_{0.5v}$) [12,14]. The plots suggested better agreement with results obtained from Wilson et al. [14] than that obtained from other studies.

Normalized temperature profile of non-isothermal plane wall jet in different positions (i.e., $x = 0.3$, 0.5, and $0.7L$) with airflow rate of 0.185 cms and $\Delta T = 40\,^{\circ}C$ are presented in Fig. 7(B). Both the predicted expressions of Wilson et al. [14] and Albright and Scott [15] showed similar agreement for experimental data than that of Grimitlyn and Pozin [12]. The shape of temperature profile is similar as velocity profile.

4.4. Airflow boundary layer growth and thermal boundary layer growth

The position data of half the maximum airspeed of air-jet with various airflow rates in both isothermal and non-isothermal conditions are described in Fig. 8(A). The root mean-square error (RMSE) between experimental data and Rajaratnam's prediction was 2.45, which was less than that of Sigalla (3.96), Liu et al. (5.86), and Albright (4.55). The experimental data had the best agreement with Rajaratnam [16] compared with other studies [17,25,26] that all the predicted expressions were derived from an isothermal air-jet. The growth of thermal boundary layer, which indicated by the vertical distance where the temperature difference is half of the extreme temperature difference, is shown in Fig. 8(B). Both the predicted curves from Albright and Scott [15] and Wilson et al. [14] fitted well with the experimental data and the RMSE were 3.63 and 3.13, respectively. The rate of growth decreased when the air-jet traveled close to the opposite wall inside an enclosure.

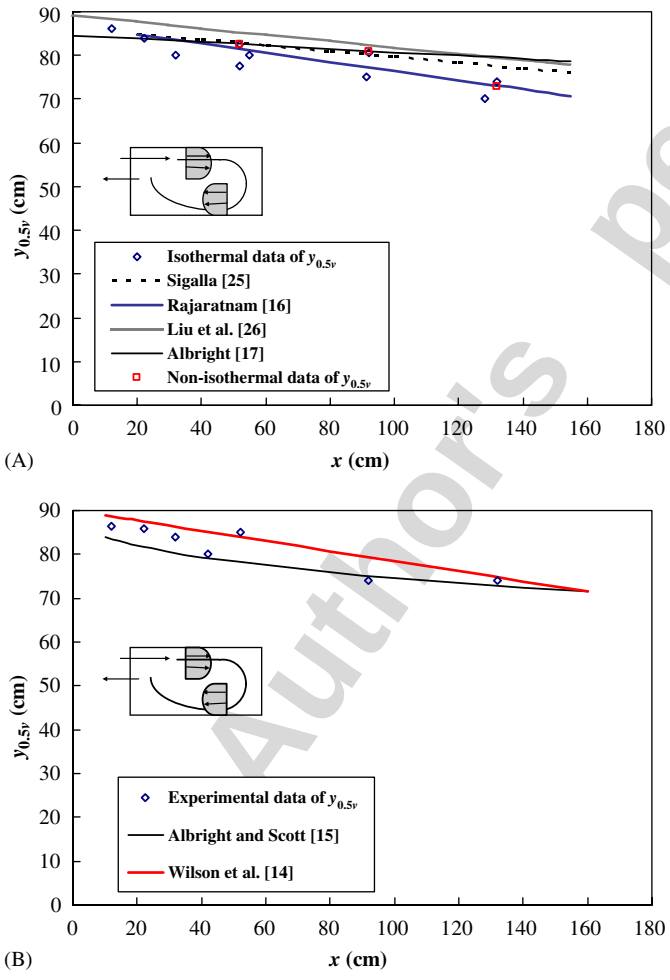

Fig. 8. Position of (A) half of the extreme airspeed and (B) half of the extreme temperature difference along enclosure ceiling.

4.5. Floor velocity and floor temperature

The maximum floor velocity was fitted well with jet momentum (M), jet momentum number (J), and inlet jet

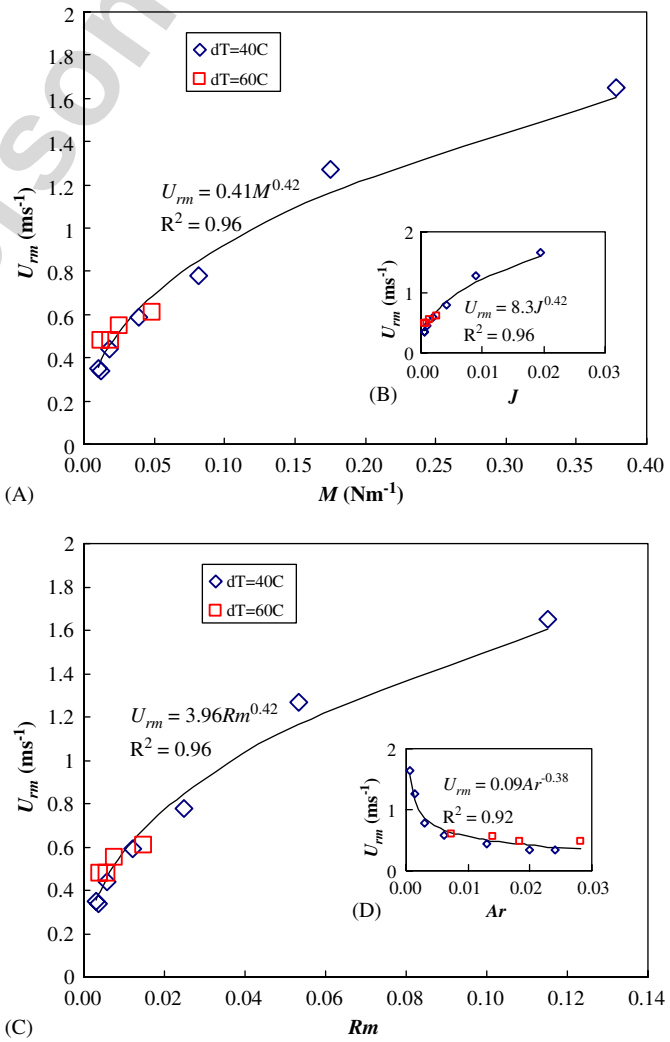

Fig. 9. Maximum floor velocity (U_{rm}) fitted with (A) jet momentum (M), (B) jet momentum number (J), (C) inlet jet momentum ratio (Rm), and (D) Archimedes number (Ar).

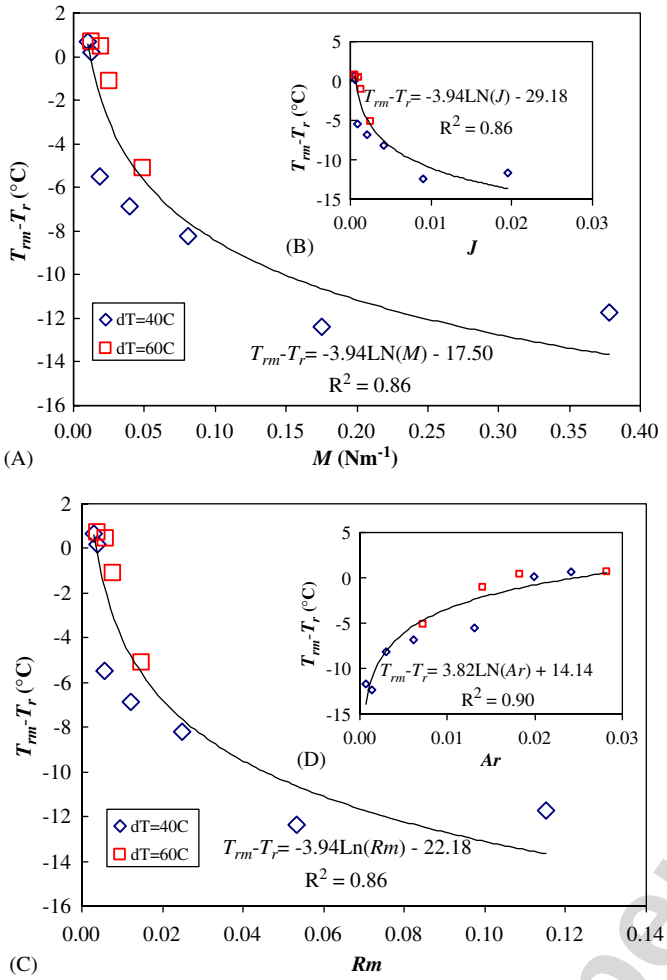

Fig. 10. Maximum temperature difference ($T_{rm} - T_r$) fitted with (A) jet momentum (M), (B) jet momentum number (J), (C) inlet jet momentum ratio (Rm), and (D) Archimedes number (Ar).

momentum ratio (Rm) (Figs. 9(A–C)). All the parameters relating to the inertia force resulted in same coefficient of determination ($r^2 = 0.96$). The maximum floor velocity also fitted well with Ar that was the ratio of buoyancy to viscosity (Fig. 9(D)). An expression followed the results of Wang and Ogilvie [9] was fitted as following:

$$U_{rm} = 4.71\sqrt{R_m} + 0.0023(H\Delta T), \quad (r^2 = 0.98). \tag{8}$$

The results of maximum floor velocity related to inertia force with different temperature environment were not recognized because of the temperature difference was not significant in the experiments (i.e., $\Delta T = 40$ and $60\,^{\circ}C$). The maximum floor velocity related to Ar [11] or $H\Delta T$ [9] is reasonable because the consideration of thermal environment. The temperature difference between maximum jet temperature on the floor and room temperature was fitted well with jet momentum (M), jet momentum number (J), and inlet jet momentum ratio (Rm), and Ar (Figs. 10(A–D)). Ar relating to buoyancy and viscosity has better correlation with temperature difference than other parameters relating to inertia force only.

5. Conclusions

The airflow characteristics of plane wall jet diffused from ceiling slot-inlet into a non-isothermal enclosure were investigated through the scale-model study. The results showed that the air-jet behavior was similar as an isothermal plane wall jet while the airflow rate beyond a critical value (i.e., $Ar < 0.004$) and inertia force dominate airflow pattern as pseudo-isothermal air-jet. When the airflow condition below a critical condition (i.e., $Ar > 0.018$), air-jet fell on entry immediately with buoyancy dominate airflow pattern. Intermediate condition includes single circulation air-jet (i.e., $0.004 < Ar < 0.011$) and two-circulation air-jet (i.e., $0.011 < Ar < 0.018$). The penetration distance can be fitted well with Ar when $Ar > 0.004$. The expression of centerline velocity decay for non-isothermal air-jet in ceiling region has same expression of an isothermal condition. But the rate of centerline airspeed decay in a non-isothermal floor air-jet was less than in an isothermal condition for the buoyancy effect.

The present derived predictive equations can simulate the centerline temperature decay of non-isothermal air-jet well in ceiling region. The temperature decay in the floor region was not significant because of the well-mixed reverse air-jet and the occurrence of floor heat. Both normalized velocity and normalized temperature profiles can be fitted well by predictive equations of Wilson et al. [14]. The growth of airflow boundary layer and thermal boundary layer increased positively with traveling distance of air-jet. The growth rate of airflow boundary layer in non-isothermal air-jet is similar as in the isothermal condition.

Maximum floor velocity and floor temperature difference can be fitted well with key parameters. Parameters include Ar and $H\Delta T$ are more reasonable for the effect of thermal environment. Our results demonstrate that not only the experimental data fitted well with predictive equations obtained from previous researches but also the present derived semi-empirical equations can predict well the airflow characteristics of plane wall jet in a ceiling slot-inlet ventilated non-isothermal enclosure. Our findings also identify the reality of air-jet performance in a confined enclosure.

References

[1] Szucs E. Similitude and modeling. Amsterdam, Netherlands: Elsevier Scientific Publishing Co.; 1980.
[2] Kirkpatrick A, Malmstrom T, Knappmiller K, Hittle D, Miller P, Hassani V, Anderson R. Use of low temperature air for cooling of buildings. In: Proceedings 1991 building simulation conference; 1991.
[3] Hassani V, Malmstrom T, Kirkpatrick AT. Indoor thermal environment of cold air distribution systems. ASHRAE Transactions 1993;99(1):1359–65.
[4] Li ZH, Zhang JS, Zhivov AM, Christianson LL. Characteristics of diffuser air jets and airflow in the occupied regions of mechanically ventilated rooms-a literature review. ASHRAE Transactions 1993;99(1):1119–27.

[5] Zhang G, Morsing S, Strom JS. Modeling jet drop distance for control of a nonisothermal, flat-adjusted ventilation jet. Transactions of the ASAE 1996;39(4):1421–31.
[6] Adre N, Albright LD. Criterion for establishing similar air flow patterns (isothermal) in slotted-inlet ventilated enclosures. Transactions of the ASAE 1994;37(1):235–50.
[7] Kaul P, Maltry W, Muller HJ, Winter V. Scientific-technical principles for the control of the environment in livestock houses and stores. Translation 430. N.I.A.E., Silsoe, England: British Society of Research in Agricultural Engineering; 1975.
[8] Randall JM, Battams VA. Stability criteria for airflow patterns in livestock buildings. Journal of Agricultural Engineering Research 1979;24:361–74.
[9] Wang J, Ogilvie JR. Design guidelines for floor velocity distribution in slot-inlet ventilated buildings. Paper No. 94-4536, St. Joseph, MI: American Society of Agricultural Engineers; 1994.
[10] Zhang JS. A fundamental study of two dimensional room ventilation flows under isothermal and non-isothermal conditions. Unpublished PhD dissertation, University of Illinois at Urbana-Champaign, Urbana, IL, 1991.
[11] Zhang JS, Christianson LL, Riskowski GL. Regional airflow characteristics in a mechanically ventilated room under non-isothermal conditions. ASHRAE Transactions 1990;96(1):751–9.
[12] Grimitlyn MI, Pozin GM. Fundamentals of optimizing air distribution in ventilated spaces. ASHRAE Transactions 1993;93(1):1128–38.
[13] Awbi HB. Ventilation of buildings. London: Chapman & Hall; 1991.
[14] Wilson JD, Esmay ML, Persson S. Wall-jet velocity and temperature profiles resulting from a ventilation inlet. Transactions of the ASAE 1970;13(1):77–81.
[15] Albright LD, Scott NR. The low-speed non-isothermal wall jet. Journal of Agricultural Engineering Research 1974;19:25–34.
[16] Rajaratnam N. Turbulent jets. Amsterdam, Netherlands: Elsevier Scientific Publishing Co.; 1976.
[17] Albright LD. Environmental control for animals and plants. St. Joseph, MI: American Society of Agricultural Engineers; 1990.
[18] Etheridge D, Sandberg M. Building ventilation: theory and measurement. New York: Wiley; 1996.
[19] Forthmann E. Turbulent jet expansion. Technical memorandum no. 789. National Advisory Committee for Aeronautics, USA, 1934.
[20] Thorshauge J. Air-velocity fluctuations in the occupied zone of ventilated spaces. ASHRAE Transactions 1982;88(2):753–64.
[21] Rodahl E. The point of separation for cold jets flowing along the ceiling. CLIMA 2000, Belgrade, Yugoslavia, 1977.
[22] Yu H, Liao CM, Liang HM. Scale model study of airflow performance in a ceiling slot-ventilated enclosure: isothermal condition. Building and Environment 2003;38:1271–9.
[23] ASHRAE. ASHRAE handbook: fundamentals. Atlanta, GA: American Society of Heating, Refrigeration and Air-Conditioning Engineers; 1993.
[24] Shepelev I. Air supply ventilation jets and air fountains. In: Proceedings of the academy of construction and architecture of the USSR 4. 1961.
[25] Sigalla A. Measurements of skin friction in a plane turbulent wall jet. Journal of Agricultural Engineering Research 1958;6:873–7.
[26] Liu Q, Hoff SJ, Maxwell GM, Bundy DS. A numerical study of slotted wall jets with and without ceiling. ASAE paper no. 944583, St. Joseph, MI: American Society of Agricultural Engineers; 1994.